

## Sulforaphene promotes Bax/Bcl2, MAPK-dependent human gastric cancer AGS cells apoptosis and inhibits migration *via* EGFR, p-ERK1/2 down-regulation

Arindam Mondal<sup>1</sup>, Raktim Biswas<sup>1,3</sup>, Yun-Hee Rhee<sup>1</sup>, Jongkee Kim<sup>2</sup> and Jin-Chul Ahn<sup>1,3</sup>

<sup>1</sup> Beckman Laser Institute Korea, Dankook University, 119, Dandae-ro, Cheonan, Chungnam, 330-714, Republic of Korea

<sup>2</sup> Department of Integrative Plant Science, Chung-ang University, Ansong, 456-756, Republic of Korea

<sup>3</sup> Department of Biomedical Science, College of Medicine, Dankook University, 119, Anseo-dong, Cheonan, Chungnam, 330-714, Republic of Korea

**Abstract.** Gastric cancer migration and invasion considered as main causes of this cancer-related death around the world. Sulforaphene (4-isothiocyanato-4R-(methylsulfinyl)-1-butene), a structural analog of sulforaphane, has been found to exhibit anticancer potential against different cancers. Our aim was to investigate whether dietary isothiocyanate sulforaphene (SFE) can promote human gastric cancer (AGS) cells apoptosis and inhibit migration. Cells were treated with various concentrations of SFE and cell viability, morphology, intracellular ROS, migration and different signaling protein expressions were investigated. The results indicate that SFE decreases AGS cell viability and induces apoptosis in a dose-dependent manner. Intracellular ROS generation, dose- and time-dependent Bax/Bcl2 alteration and signaling proteins like cytochrome c, Casp-3, Casp-8 and PARP-1 higher expression demonstrated the SFE-induced apoptotic pathway in AGS cells. Again, SFE induced apoptosis also accompanied by the phosphorylation of mitogen-activated protein kinases (MAPKs) like JNK and P-38. Moreover, dose-dependent EGFR, p-ERK1/2 down-regulation and cell migration inhibition at non-toxic concentration confirms SFE activity in AGS cell migration inhibition. Thus, this study demonstrated effective chemotherapeutic potential of SFE by inducing apoptosis as well as inhibiting migration and their preliminary mechanism for human gastric cancer management.

**Key words:** Sulforaphene — Gastric cancer — Apoptosis — Migration inhibition — MAPKs

### Introduction

A diet containing isothiocyanate (ITC)-rich cruciferous vegetables has higher potency against various malignancies, such as liver, prostate, ovary, lung, colon and gastrointestinal tract carcinoma (Giovannucci et al. 2003; Lam et al. 2009; Powolny et al. 2011; Wu et al. 2011; Bosetti et al. 2012; Razis and Noor 2013; Gupta et al. 2014). ITCs are formed by the hydrolysis of precursor glucosinolates by myrosinase enzyme (Fahey et al. 2012). Previous studies reported that due to higher ligand binding affinity, ITC can easily bind to the specific target in the human body and exhibit their efficacy in cellular apop-

toxis against various cancer cells *in vitro* and *in vivo* (Mi et al. 2008). Sulforaphene (4-isothiocyanato-4R-(methylsulfinyl)-1-butene) is one of the major anticancer agents present in radish and structural analog of sulforaphane (Kaur 2009). Sulforaphene (SFE) possess antimicrobial and antiviral effects along with antioxidative effects in rat carcinogenesis. It can not only reduce cancer cell proliferation in a dose-dependent manner, but also induce apoptosis in LoVo, HCT-116 and HT-29 cancer cells (Barillari et al. 2008; Papi et al. 2008; Pocasap et al. 2013). SFE is also reported as one of the most potent inhibitor of food-derived heterocyclic amine-induced bacterial mutagenesis in TA100 (Kaur 2009). Moreover, the toxicity of SFE on normal T-lymphocytes were reported to be negligible, which indicates minimum side effects of SFE on normal cells (Barillari et al. 2008; Papi et al. 2008).

The incidence of gastric cancer is very high in East Asia, including Korea and Japan (Inoue and Tsugane 2005; Leung

Correspondence to: Jin Chul Ahn, Beckman Laser Institute Korea, College of Medicine, Dankook University, 119, Dandae-ro, Cheonan, Chungnam, 330-714, Republic of Korea  
E-mail: jcahn@dankook.ac.kr

et al. 2008; Hartgrink et al. 2009). Although chemotherapy and surgery have been found to be effective in gastric cancer treatment, but the invasion and metastasis of cancer cells remain the primary cause of gastric cancer-related death (Gotoda et al. 2000). Therefore, it is essential to find out a novel anticancer agent which not only induce apoptosis in cancer cells, but also inhibit cell proliferation, invasion and metastasis without any adverse effect. The extracellular signal-regulated kinase (ERK) and epidermal growth factor receptor (EGFR) play important roles in cancer cell survival and proliferation along with invasion and metastasis. On the other hand, down-regulation of Bcl2, up-regulation of Bax and other pathway-related proteins are involved in apoptotic mechanism. Phosphorylation of c-Jun N-terminal kinase (JNK) and P-38 also play important role in cellular apoptosis (Choi and Singh 2005; Yan et al. 2011; Avisetti et al. 2014).

Our present study designed to investigate dietary isothiocyanate SFE-induced cellular apoptosis along with inhibition of cancer cell migration in human gastric cancer cells (AGS). Cells were treated with various concentrations of SFE and dose-dependent apoptosis induction was investigated. Besides this, different signaling proteins were studied to find out possible mechanism of apoptosis. We also investigated the cell migration inhibition efficacy of SFE. Therefore, this study has a broad potential for the management of human gastric cancer by inducing apoptosis and inhibiting cell migration.

## Materials and Methods

### Chemicals

S-Sulforaphene was purchased from LKT Laboratories, Inc, USA. 3-[4,5-dimethylthiazol-2-yl] -2,5-diphenyl-tetrazolium bromide (MTT), dimethyl sulfoxide (DMSO), Hoechst33342, propidium iodide (PI), RIPA buffer, protease and phosphatase inhibitors were purchased from Sigma (Saint Louis, MO, USA). H<sub>2</sub>DCF-DA (2',7'-Dichlorodihydrofluorescein diacetate) was obtained from Invitrogen (Eugene, OR, United States). Bradford Reagent was supplied by Bio-Rad (Hercules, CA, USA). Poly (ADP-Ribose) polymerase (PARP), casp-3, p-P 38 were purchased from cell signaling technology (Beverly, MA, USA). Bax, Bcl2, Cytochrome c, casp-8, EGFR, ERK1/2, p-ERK1/2, JNK, p-JNK and  $\beta$ -actin were purchased from Santa Cruz Biotechnology, Inc (Santa Cruz, CA, USA).

### Preparation of sulforaphene stock solution

50 mg/ml stock solution was prepared by dissolving S-Sulforaphene in Dulbecco's phosphate-buffered saline (DPBS)

(Welgene, Daegu, South Korea) and stored at  $-20^{\circ}\text{C}$  in dark condition. Before treatment, SFE was diluted in culture medium according to required specific concentration.

### Cell culture

AGS cell was purchased from Korean cell line bank and cultured in RPMI media (HyClone, South Logan, UT) supplemented with 10% fetal bovine serum (FBS) (Equitech-Bio Inc, Texas) and 1% streptomycin/penicillin (Gibco, BRL). The cells maintained at  $37^{\circ}\text{C}$  in a 5% CO<sub>2</sub> humidified environment. All the cell culture dish was from SPL Life Science (Pocheon, South Korea).

### Cytotoxicity assay

AGS cells were inoculated into a 96-well, flat-bottomed microplate at a volume of 100  $\mu\text{l}$  ( $1 \times 10^5$  cells/ml) for a stationary culture and incubated overnight in growth medium to allow the cells to adhere the bottom of wells. The media was replaced with a new fresh media and the cells were treated with a series of SFE starting from 0  $\mu\text{g/ml}$  to 100  $\mu\text{g/ml}$ . Treated cells were incubated for 3, 6, 12 and 24 h in 5% CO<sub>2</sub> at  $37^{\circ}\text{C}$ . After incubation, 50  $\mu\text{l}$  MTT solution (2 mg/ml) was added to each well. 4 h after incubation in 5% CO<sub>2</sub> at  $37^{\circ}\text{C}$ , media of each well was removed and 150  $\mu\text{l}$  DMSO was added to dissolve violet blue crystals. The cytotoxic effect of SFE on the growth of AGS cells was determined by measuring the absorbance at 570 nm using ELISA reader (Biochrom, UK).

### Microscopic analysis of cell morphology

AGS cells were treated with 2, 3.5, 5.5  $\mu\text{g/ml}$  concentrations of SFE and were incubated for 24 h. The concurrent appearances of the AGS cells, after treatment were observed through an inverted microscope (Olympus CK40, Japan). The morphology of the control cells and treated cells were observed and the photographs were taken.

### Apoptosis assay

To measure the morphological changes of the nuclear chromatin inducing apoptosis in AGS cells, Hoechst 33342 staining was performed. Cells were seeded in 6 well plates and treated with 2, 3.5 and 5.5  $\mu\text{g/ml}$  SFE and incubated for 24 h in 5% CO<sub>2</sub> at  $37^{\circ}\text{C}$ . The cells were incubated with Hoechst 33342 (1  $\mu\text{g/ml}$ ) for 30 minutes. The stained cells were observed to assess the cellular apoptosis using a confocal microscope (Zeiss, 510 Meta, Germany) under equivalent set of conditions, respectively. A histogram was prepared to compare the percentage of increase of apoptotic cells, in different treatment groups.

### *Analysis of intracellular ROS generation*

To analyze SFE-induced intracellular ROS generation in AGS cells after treatment, H<sub>2</sub>DCF-DA was used as the oxidant sensitive fluorescent probe. The cells were treated with 2, 3.5 and 5.5 µg/ml SFE as mentioned previously, and incubated for 24 h in 5% CO<sub>2</sub> at 37°C. 20 µM of H<sub>2</sub>DCF-DA in pre-incubated DPBS was added for 30 minutes at 37°C. The relative intensities of green fluorescence in treatment samples were measured using a confocal microscope (Zeiss, 510 Meta, Germany) at 488 nm excitation wavelength under equivalent conditions. A histogram was prepared to compare relative fluorescence intensities of different treatment groups with control group.

### *Expression of apoptotic pathway related and cell survival proteins by Western blot analysis*

The expressions of apoptosis signalling and cell migration proteins were analyzed by Western blot technique. AGS cells were treated with 2, 3.5 and 5.5 µg/ml SFE for 24 h. Then the cells were washed with DPBS twice and the proteins were extracted in RIPA buffer (50 mM Tris-HCl, pH 8.0, 1% NP-40, 0.5% sodium deoxycholate, 150 mM NaCl, and 0.1% sodium dodecyl sulfate with protease and phosphatase inhibitor cocktail (Sigma, MO)) and centrifuged at 15,000 rpm for 30 minutes at 4°C. The protein concentration was determined using the Bradford Protein Assay Reagent. Equivalent amounts of protein from each sample were loaded onto polyacrylamide gels and separated by electrophoresis. Then the proteins were transferred to PVDF membranes (Immuno-Blot PVDF, BioRad Laboratories, Hercules, USA). Both electrophoresis and blotting were performed by using a PowerPac200 electrophoresis system (BioRad Laboratories, Hercules, USA). The membranes were then blocked for 2 h at room temperature in Tris-buffered saline containing 0.1% Tween-20 and 5% BSA. Then membrane was incubated overnight at 4°C with the primary antibody diluted with 3% BSA on a multishaker. The membranes were probed with horseradish peroxidase-conjugated anti-mouse IgG, anti-goat IgG or anti-rabbit IgG antibody for 2 h. The protein band was developed by ECL Western Blotting detection reagents (GE Healthcare, Buckinghamshire, UK) and the pictures were taken by Kodak in vivo image analyzer (Eastern Kodak, Rochester, NY, USA).

### *Cell migration assay*

The *in vitro* AGS cells migration inhibition efficacy of SFE was investigated according to Liang et al. (2007). To investigate this, first 10<sup>5</sup> cells were grown in 60 mm cell culture dishes and allowed upto 70% confluence.

A “lesion” was created on the monolayer of cells with a p200 pipette tip in each cell culture dish and washed with DPBS to remove the debris. Then the culture dishes were divided into two groups; control group and SFE treatment group. In control group, only fresh media was added and in SFE treatment group the cells were treated with 1.5 µg/ml SFE in fresh media. From MTT assay at 1.5 µg/ml, the AGS cell viability was approximately more than 90% after 24 h SFE treatment which indicates that this concentration of SFE is comparatively non-toxic to AGS cells. Then the cells were incubated for 3, 6, 12, 24 h in 5% CO<sub>2</sub> at 37°C. The images of the lesions were taken through a phase-contrast microscope before the treatment as well as after 3, 6, 12 and 24 h incubation. The distances between one side of the scratch to the other side were quantitatively measured by Image J software (NIH, USA). The percentage of average cell migration at 3, 6, 12 and 24 h in both control and SFE-treated groups were compared by comparing the distances between one side of the “lesion” to the other side with that of pretreatment “lesion”. A histogram was prepared to show the percentage of AGS cell migration with and without SFE treatment at different intervals of time.

### *Statistical analysis*

All data were expressed as the mean ± SE of three independent experiments. Differences between control and treated groups were analysed using the Newman-Keuls one-way ANOVA. \*  $p < 0.05$ , \*\*  $p < 0.01$  and \*\*\*  $p < 0.001$  were considered statistically significant.

## **Results**

### *SFE reduces the viability of AGS cells*

Figure 1A indicates that SFE can inhibit the growth of AGS cell in a dose- and time-dependent manner. The MTT assay results indicate that percentage of AGS cell viability decreases at higher concentrations and different incubation time after SFE treatment. Cells treated with SFE for 3 h showed approx. 98% and 93% cell viabilities at 3.2 µg/ml and 6.75 µg/ml of SFE, respectively, whereas at the same concentration, the percentages of cell viabilities were approx. 98% and 82% at 6 h SFE treatment, and approx. 81% and 58% at 12 h treatment, respectively. On the other hand, approx. 75% and 25% cells were viable in 24 h of SFE treatment at concentrations of 3.2 µg/ml and 6.75 µg/ml, respectively. From the MTT assay, 2.0, 3.5 and 5.5 µg/ml of SFE, which showed approx. 80% to 50% cell viability decrease after 24 h incubation, were selected to be used in further experiments as SFE concentration.

### SFE changes the morphology of AGS cells

The morphology of the AGS cell was observed after SFE treatment and the cellular morphology was compared with control (no SFE treatment) through inverted microscope. Microscopic images (Figure 1B) indicate that most of the cells were attached to the bottom of the culture flask with normal cell morphology in the control. But at higher concentration of SFE (3.5, 5.5  $\mu\text{g/ml}$ ) treatment, maximum number of cells were detached from bottom of the culture flask. The morphology of the treated cells was also changed

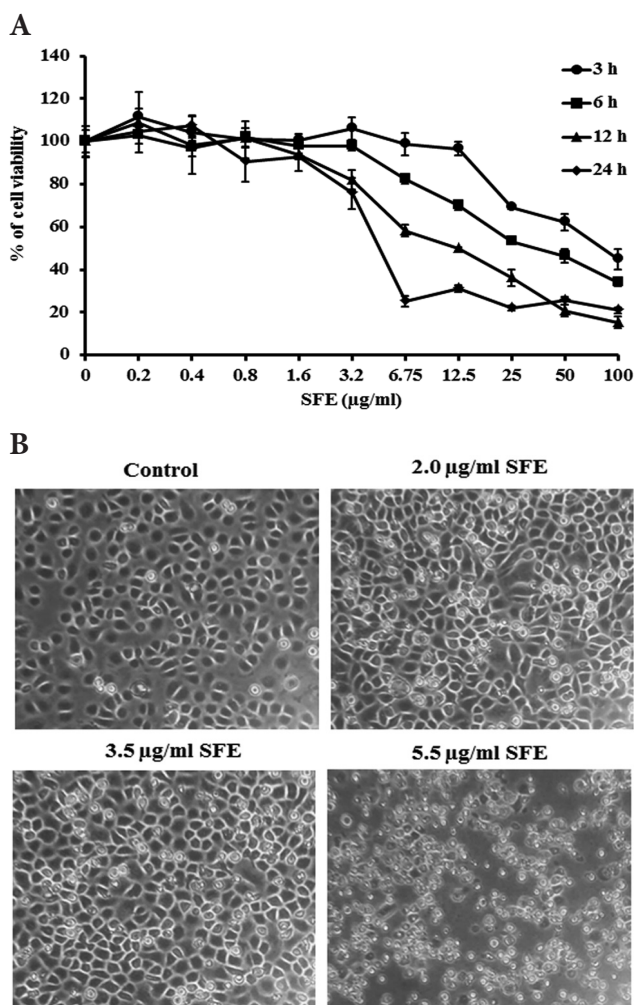


**Figure 1.** A. MTT assay of AGS cells treated with a series of SFE concentration and incubated for 3, 6, 12 and 24 h. Cell viability decreased with increasing concentration of SFE as well as increasing time interval. B. Inverted microscopic images (magnification  $\times 10$ ) of AGS cells after treatment with 2, 3.5 and 5.5  $\mu\text{g/ml}$  of SFE for 24 h. Control cells show normal cell morphology and as the concentration increases cell became round shaped and started to detach from the bottom of the culture flask. At 5.5  $\mu\text{g/ml}$  concentration maximum cells were round shaped.

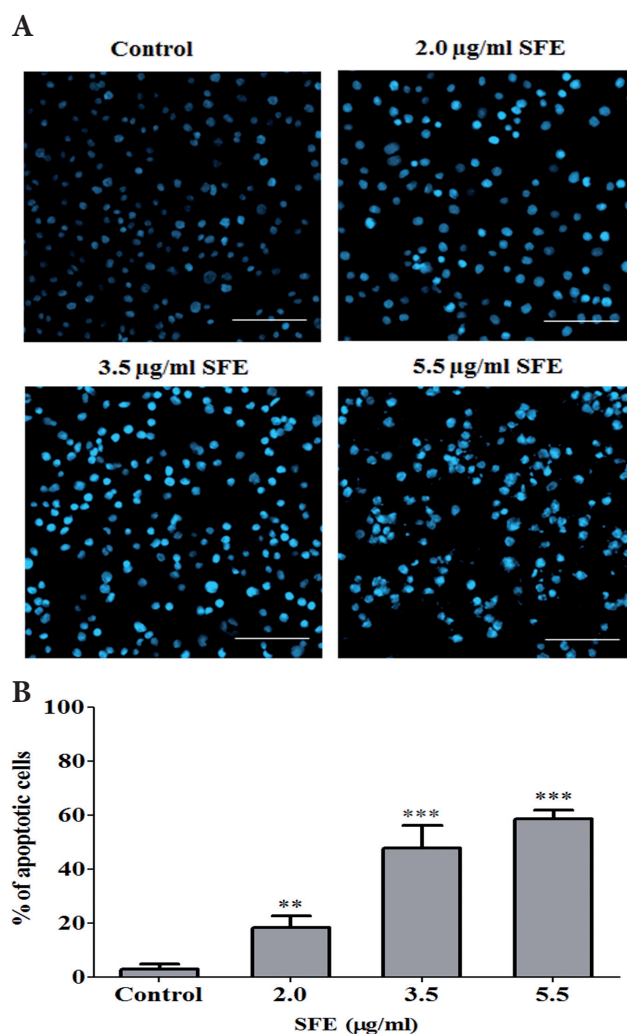


**Figure 2.** A. Hoechst 33342 staining in AGS cells for control and treatment with 2, 3.5 and 5.5  $\mu\text{g/ml}$  of SFE for 24 h. Apoptotic cells with bright fluorescence increases with the increase in SFE concentration. The scale bar indicates 100  $\mu\text{m}$ . B. Histogram represents the percentage of apoptotic cells in different treatment concentrations. At each treatment concentration percentage of apoptotic cells increases significantly with respect to control. \*\*  $p < 0.01$ , \*\*\*  $p < 0.001$ .

into round-shaped compared to the control cells. With the increase of SFE concentration, the number of round shaped cells increases and started detaching from the bottom of the culture flask. At 5.5  $\mu\text{g/ml}$  SFE concentration, maximum cells were found to be round shaped.

### SFE induces apoptosis in AGS cells

Dose-dependent apoptosis and doses selected for further experiments of SFE against AGS cell was confirmed by staining the cells with Hoechst 33342. Microscopic images (Figure 2A) demonstrates the shrunken nucleus and

fragmented chromatin after SFE treatment. Apoptotic cells were found to show bright fluorescence whereas the normal cells show lower fluorescence. The fluorescence photomicrographs also indicate that upon SFE treatment percentage of apoptotic cells were increased. The percentage of apoptotic cells in different treatment concentrations were represented by a histogram (Figure 2B). The percentage of apoptotic cells are much less in 2  $\mu\text{g}/\text{ml}$  but significantly increases at 3.5 and 5.5  $\mu\text{g}/\text{ml}$  of SFE concentrations. Maximum cells present at 5.5  $\mu\text{g}/\text{ml}$  of SFE were found to be apoptotic in nature.

#### *SFE induces apoptosis by generating intracellular ROS*

Confocal microscopic images and relative fluorescence intensity histogram (Figure 3) indicate that SFE treatment generate intracellular ROS in AGS cells. H2DCFDA-derived fluorescence intensity was minimal in cells without SFE treatment. Although at 2  $\mu\text{g}/\text{ml}$  concentration, the increase of fluorescence intensity is less, significant increase in fluorescence intensity was observed at 3.5 and 5.5  $\mu\text{g}/\text{ml}$  SFE. The fluorescence intensity was found higher in 3.5  $\mu\text{g}/\text{ml}$  of SFE treatment than other treatment groups. Histogram represents relative change in fluorescence levels at different concentrations of SFE.

#### *Dose- and time-dependent modulation of Bax and Bcl2 by SFE treatment*

Generation of ROS in cancer cell is also associated with Bax up-regulation. So we investigated dose- and time-dependent Bax and Bcl2 alteration. Western blot analysis (Figure 4A) shows a significant time-dependent increase in Bax expression and significant decrease in Bcl2 expression in 0, 3, 6, 12 and 24 h after 5.5  $\mu\text{g}/\text{ml}$  SFE treatment, respectively. Significant up-regulation of Bax and down-regulation of Bcl2 was observed with maximum at 24 h of SFE treatment. On the other hand, at 24 hours, Bax expression also increases with the increase of SFE concentration; the highest expression was observed at 5.5  $\mu\text{g}/\text{ml}$  SFE concentration. Consequently the expression of Bcl2 was also down-regulated dose-dependently and at 5.5  $\mu\text{g}/\text{ml}$  of SFE concentration, Bcl2 expression was found to be minimal (Figure 4C). Histogram (Figure 4B,D) represents relative alteration of Bax and Bcl2 interms of band intensity.

#### *SFE treatment modulates apoptotic signaling proteins*

SFE treatment modulates apoptotic signaling proteins like cyt-c, casp-8, casp-3, and PARP-1 in AGS cells in dose-dependent manner. Protein expressions in Western blot analysis (Figure 4A) show higher expression of cyt-c after

SFE treatment. Casp-8 and PARP-1 were found to be cleaved and expressed highest at 5.5  $\mu\text{g}/\text{ml}$  of SFE treatment. Casp-3 was also found to be up-regulated with the increase of SFE treatment. Histogram (Figure 4B) represents relative modulation of cyt-c, cleaved casp-8, casp-3, and cleaved PARP-1 interms of their band intensity.

#### *SFE treatment modulates MAPKs for AGS cell apoptosis*

SFE treatment also found to be responsible in phosphorylation of different mitogen-activated protein kinases. Western blot analysis showed that the expressions of p-JNK and

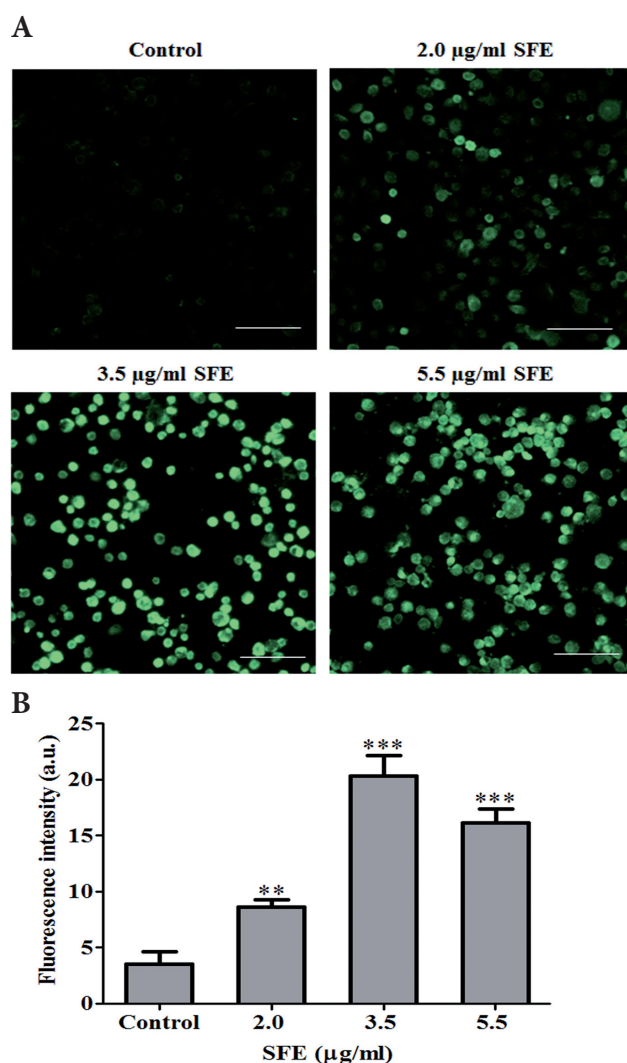


**Figure 3.** A. Generation of intracellular ROS after treatment of 3.5 and 5.5  $\mu\text{g}/\text{ml}$  of SFE for 24 h. SFE treatment increases H2DCFDA-derived fluorescence levels in AGS cells. The scale bar indicates 100  $\mu\text{m}$ . B. Histogram represents the changes in H2DCFDA-derived fluorescence levels at different concentrations of SFE. \*\*  $p < 0.01$ , \*\*\*  $p < 0.001$ .

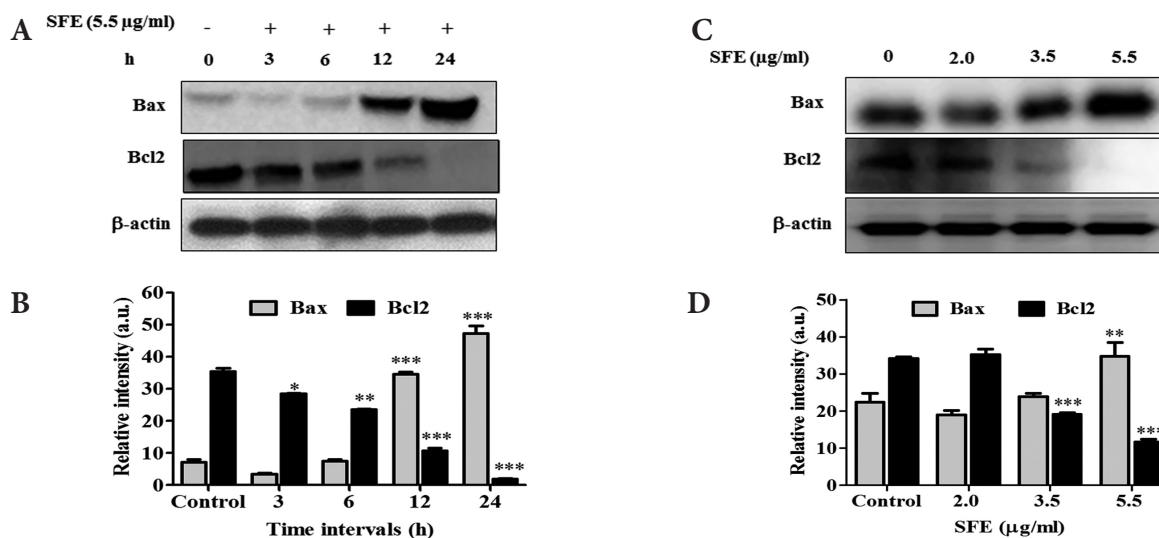


**Figure 4.** A. Western blot analysis for alteration expressions of Bax and Bcl2 after 5.5 µg/ml SFE treatment in AGS cells for 3, 6, 12 and 24 h. The expression of Bax increases with time and Bcl2 expression decreases consequently. The highest Bax expression and the lowest Bcl2 expression was observed at 24 h. B. Histogram represents the alteration of Bax and Bcl2 expression in different time interval. C. Alteration Bax and Bcl2 after treatment with 2, 3.5 and 5.5 µg/ml of SFE for 24 h. Up-regulation of Bax and consequent down-regulation of Bcl2 occurs with the increase of treatment concentration. D. Histogram represents the modulation of Bax and Bcl2 expression at different concentration of SFE after 24 h treatment. \*\*  $p < 0.01$ , \*\*\*  $p < 0.001$ .

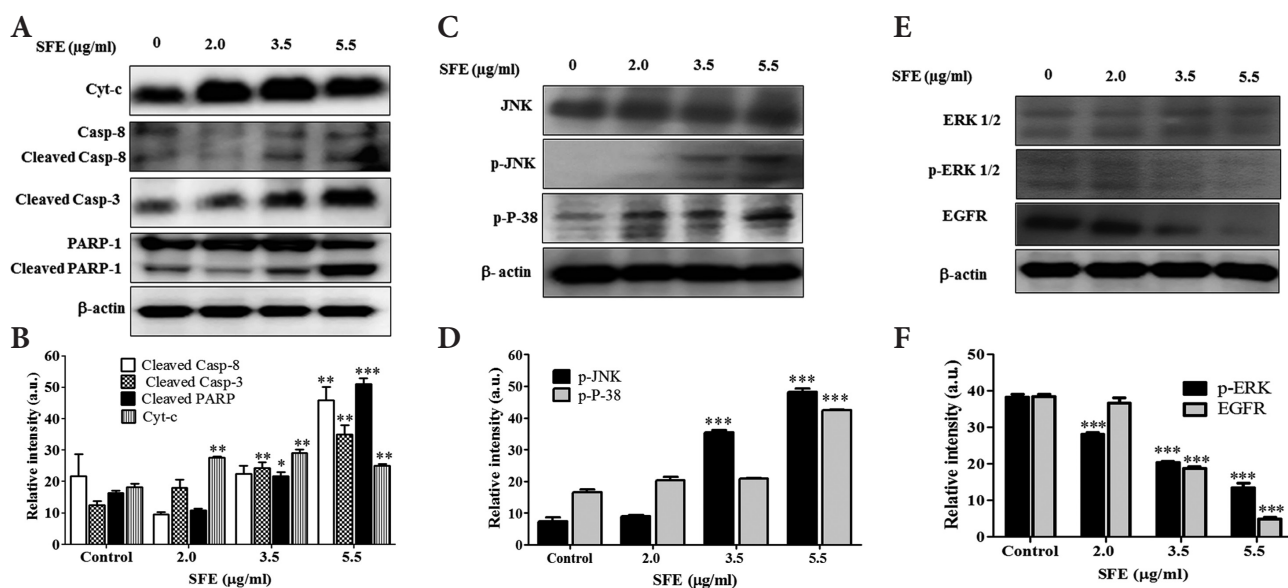


**Figure 5.** A. Western blot analysis of cyt-c, casp-8, casp-3 and PARP-1 expressions in AGS cells treated with 2, 3.5 and 5.5 µg/ml of SFE for 24 h. Expressions of all the proteins were up-regulated with increasing concentrations of SFE. Higher expression of all the proteins was observed at higher treatment concentration. B. Histogram represents relative modulation of cyt-c, cleaved casp-8, cleaved casp-3, and cleaved PARP-1 after SFE treatment interms of their band intensity. C. Expressions of JNK, p-JNK and p-P-38 after 24 h treatment of 2, 3.5 and 5.5 µg/ml of SFE in AGS cells by Western blot. p-JNK and p-P-38 was up-regulated with the increased SFE concentration but JNK remained unchanged. D. Histogram of p-JNK and p-P-38 modulation at different concentration of SFE interms of band intensity. E. Expressions of ERK1/2, p-ERK1/2 and EGFR after treatment of 2, 3.5 and 5.5 µg/ml of SFE. The p-ERK1/2 and EGFR were found to be down-regulated with the increase in SFE concentration. At concentration 5.5 µg/ml of SFE, the expression of these two proteins was found to be minimal. The expression of ERK1/2 was observed similar in both control and SFE-treated cells. F. Histogram represents significant decrease in p-ERK1/2 and EGFR expression interms of band intensity at different concentration of SFE treatment. \*  $p < 0.05$ , \*\*  $p < 0.01$ , \*\*\*  $p < 0.001$ .

p-P-38 were up-regulated with SFE treatment (Figure 5C). At concentration 5.5  $\mu\text{g/ml}$  of SFE, p-JNK and p-P-38 have higher expression than other treatment concentrations. Although p-JNK was found to be up-regulated, but total JNK remained similar after treatment of SFE. Histograms in Figure 5D, represents relative increase in p-JNK and p-P-38 interms of band intensity after SFE treatment.

#### SFE treatment dose dependently down-regulates EGFR and p-ERK1/2

Western blot analysis (Figure 5E) indicated that SFE treatment inhibits the phosphorylation of ERK1/2 without affecting total ERK1/2. ERK1/2 expression was observed almost similar at all concentrations of SFE, whereas p-ERK1/2 decreased significantly with the increase of SFE concentration. Histogram of Western blot band intensity (Figure 5F) showed significant decrease in p-ERK1/2 activity at different concentrations SFE.

On the othe hand, EGFR protein was also observed to be down-regulated in SFE-treated cells by Western blot analysis. Figure 5E clearly demonstrated the dose dependency in EGFR activity in AGS cells. In control and in 2.0  $\mu\text{g/ml}$  SFE-treated cells, the expression of EGFR was found to be higher than in the other treatment. In 3.5 and 5.5  $\mu\text{g/ml}$  SFE treatment, the expression of EGFR decreased significantly. Histogram of Western blot band intensity (Figure 5F) also validated the relative decrease of EGFR activity at different SFE concentrations.

#### SFE inhibits the migration of AGS cells in vitro

SFE treatment was observed to reduce the extent of AGS cell migration in all of our experimental time intervals. The cell density in the control and individual treatment groups was found similar. The differential migration of control and SFE-treated AGS cells at different time intervals were shown in Figure 6. The figures clearly demonstrate that the migrating distance of control AGS cells decreased in 0–24 h. But SFE treatment showed less migration than the control cells in 3, 6, and 12 h. However, after 24 h, most of the SFE-treated cells were observed to loose their migration property as the distance between the “lesion” was much higher whereas in control group the lesion was almost complete. Therefore SFE treatment found to suppress the migration of AGS cells even after at nontoxic SFE concentration compared to the control. The histogram in Figure 6 demonstrate that as the time increases, the percentage of AGS cells migration in the control group significantly increases. But the percentage of migration of SFE-treated cells was significantly much less than the corresponding control groups.

#### Discussion

Efficacy of isothiocyanates as chemotherapeutic agent in different cancer cell apoptosis is being discussed for last few years. Several compounds of isothiocyanate family

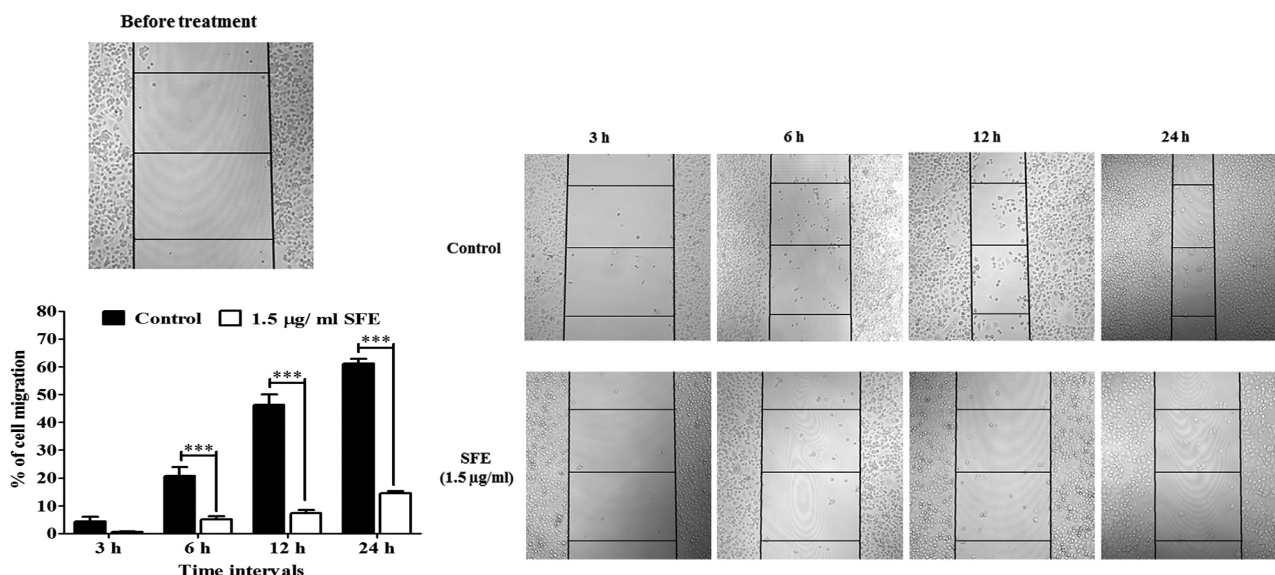


**Figure 6.** Microscopic images of cell migration assay at different time intervals. AGS cells were treated with 1.5  $\mu\text{g/ml}$  of SFE which is comparatively non-toxic to AGS cells. The cells were incubated for 3, 6, 12 and 24 h. As the time increases, the control cells migrated more into the “lesion” than the corresponding SFE-treated cells. The microscopic images and corresponding histogram represented that in control group the percentage of AGS cells migration is significantly much higher than the SFE-treated groups in all the time intervals. \*\*\*  $p < 0.001$ .

were already reported to have anticancer properties against various types of cancer (Zhang 2004; Clarke et al. 2008; Wu et al. 2009). Isothiocyanates are also reported to inhibit cell migration and invasion in gastric and other types of cancer (Yang et al. 2010; Ho et al. 2011; Yan et al. 2011). Sulforaphane is well studied multitargeted cancer preventing isothiocyanate against various types of cancer (Clarke et al. 2008). Several studies already reported sulforaphane-induced apoptosis in a wide range of cancer. But anticancer potential of SFE, one of the natural analog of sulforaphane, has not yet been studied extensively. Due to unsaturation in the alkyl chain, SFE reported to have stronger inhibitory effect against heterocyclic amines which suggest SFE to be a potential chemopreventive agent (Kaur 2009). Recent study demonstrated that sulforaphane can down-regulate Hedgehog signaling pathway to reduce breast cancer cell migration and invasion (Bao et al. 2014). On the other hand sulforaphane also reported to be effective against human colon cancer via intrinsic signal cascade and Bax/Bcl2 modulation (Papi et al. 2008). This study is the first to report that SFE can induce apoptosis in human gastric cancer cells and inhibit cancer cell migration by down-regulating EGFR and p-ERK1/2.

From the present study, cytotoxicity assay suggest that SFE has dose-and time-dependent AGS cell growth inhibition efficacy. Morphological analysis of AGS also indicates the increase of apoptotic cells after SFE treatment. When cells were stained with Hoechst 33342, the fluorescent intensity also increased in SFE-treated cells compared to control cells. The percentage of apoptotic cells were found to be increasing with the increase of SFE concentration. These results conveyed that SFE treatment inhibits AGS cells growth by inducing apoptosis. On the other hand, SFE treatment was also found to generate ROS in treated cells. This increase in ROS might damage the mitochondrial membrane potential and explore the observed higher expression of cyt-c in SFE treated cells. From Western blot data SFE treatment was found to be effective in Bax activation. Our experimental results suggest that SFE treatment is responsible for both time- and dose-dependent activation of Bax. On the other hand, Bcl2 also down-regulates in time- and dose-dependent manner after SFE treatment. Extrinsic pathway protein casp-8 and downstream protein PARP-1 were found to be cleaved and up-regulated during SFE-induced apoptosis. Dose-dependent activation of cleaved casp-3 was also observed. SFE treatment also found to be responsible for the phosphorylation of stress

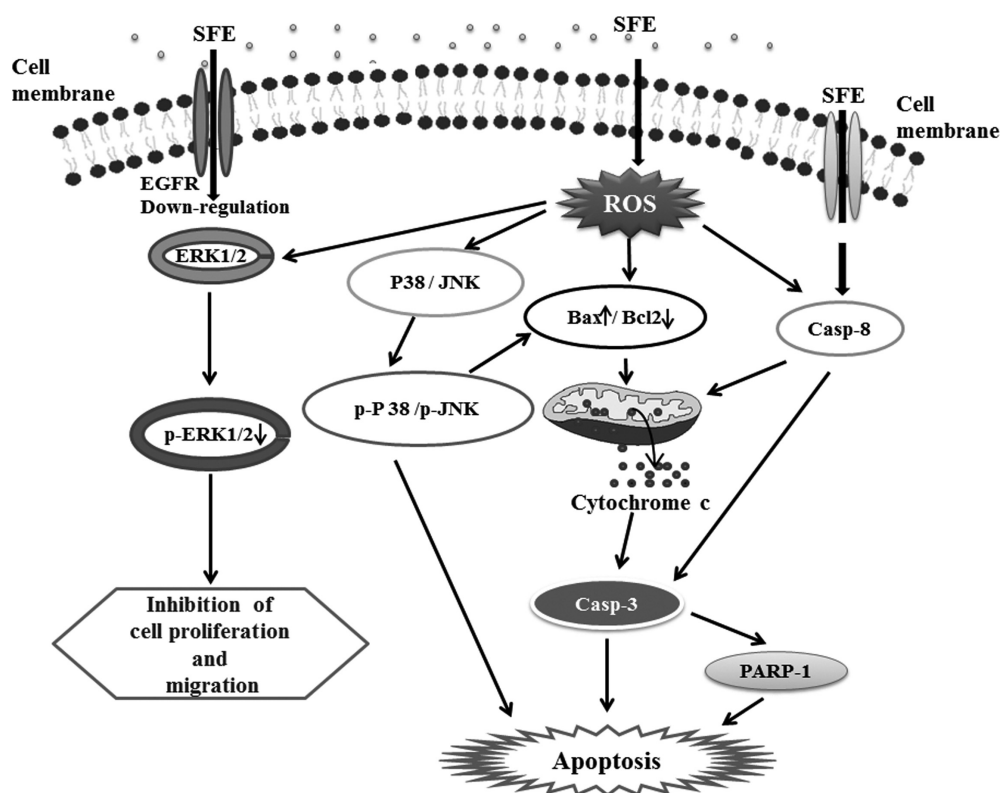


**Figure 7.** Schematic flow-diagram representing the SFE activity in AGS cells. Intracellular ROS generates after treatment of SFE which activates different apoptotic signaling proteins. Pro-apoptotic Bax up-regulation and anti-apoptotic Bcl2 down-regulation activates mitochondrial apoptotic pathway. Intrinsic pathway related cytochrome c higher expression and casp-3 activation leads to AGS cells apoptosis. Extrinsic death-receptor protein casp-8 was activated and helped in cyt c release from mitochondria to cytosol, casp-3 activation and thereby induce apoptosis. PARP-1 also cleaved and activated by SFE and induces apoptosis. Beside this, phosphorylation of JNK and P-38 from mitogen-activated protein kinases (MAPKs) leads to

Bax/ Bcl2 modulation and AGS cells apoptosis. Moreover, down-regulation EGFR and inhibition of ERK1/2 phosphorylation after SFE treatment leads to inhibition of AGS cells proliferation and migration.

and cellular damage related MAPKs such as JNK and p-38. Dose-dependent up-regulation of p-JNK and p-P-38 was observed in SFE-treated AGS cells. These activated MAPKs also help to promote Bax translocation to mitochondria (Tsuruta et al. 2004) as well as activate stress-induced mitochondrial signaling pathway of apoptosis (Tournier et al. 2000). The expression of all the apoptotic signalling proteins was observed to be increased in higher SFE concentration compared to the lower treatment concentration.

Phosphorylation of ERK1/2 and activation of p-ERK1/2 is one of the key factors in cell proliferation, apoptosis resistance, and enhanced tumor invasion and metastasis (Zhang et al. 2008; Stivarou and Patsavoudi 2015). In our experiment, SFE treatment was found to be efficient to inhibit the phosphorylation and activation of p-ERK1/2. On the other hand, down-regulation of EGFR protein also indicated the SFE activity in reducing gastric cancer cells proliferation and migration. Additionally, SFE treatment effectively lessens the migration of AGS cell *in vitro*. The reduced cell migration at lower non-toxic SFE concentration suggested that the inhibition of AGS cell migration and further functions. From our results, it can be suggested that the inhibition of AGS cell migration after SFE treatment is not only due to the cellular apoptosis but also due to the migration inhibition efficacy of SFE. Taken together, dose-dependent decrease in p-ERK1/2, EGFR activity and consequently reduction in cell migration in our experiment implies that SFE treatment effectively inhibits gastric cancer cell proliferation and migration. A schematic diagram (Figure 7) shows that SFE treatment generates intracellular ROS and modulates different pathway-related proteins to induce AGS cells apoptosis along with down-regulation of EGFR protein and inhibition of ERK1/2 phosphorylation to inhibit AGS cells proliferation and migration.

Therefore, this study indicates that dietary isothiocyanate SFE plays an important role not only in gastric cancer cell apoptosis but also in the inhibition of AGS cell migration. However, more in-depth studies including *in vivo* chemopreventive efficacy are needed for the recommendation of SFE in future, the current study preliminarily suggests that SFE could become a potent alternative treatment modality for the management of gastric cancer as well as other cases of malignant neoplastic disease.

**Acknowledgement.** This research was supported by Bio-industry Technology Development Program (grant number, 112011-052HD030), Ministry of Agriculture, Food and Rural Affairs and Leading Foreign Research Institute Recruitment Program through the National Research Foundation of Korea funded by the Ministry of Education, Science and Technology (grant number, 2012K1A4A3053142).

**Conflict of interest.** The authors have no conflict of interest to declare.

## References

- Avisetti D. R., Babu K. S., Kalivendi S. V. (2014): Activation of p38/JNK pathway is responsible for embelin induced apoptosis in lung cancer cells: Transitional role of reactive oxygen species. *PLoS One* **9**, 1–10  
<http://dx.doi.org/10.1371/journal.pone.0087050>
- Bao C., Lee J., Ko J., Park H. C., Lee H. J. (2014): Sulforaphene inhibited migration through down-regulating the Hedgehog signaling in SUM159 human breast cancer cells. (Abstract). Proc. 105th Annu. Meet. Am. Assoc. Cancer Res. 2014 Apr 5-9; San Diego, CA. Philadelphia AACR; *Cancer Res.* **74** (19 Supp, Abstract 121).  
<http://dx.doi.org/10.1158/1538-7445.am2014-121>
- Barillari J., Iori R., Papi A., Orlandi M., Bartolini G., Gabbanini S., Pedulli G. F., Valgimigli L. (2008): Kaiware Daikon (*Raphanus sativus* L.) extract: A naturally multipotent chemopreventive agent. *J. Agric. Food Chem.* **56**, 7823–7830  
<http://dx.doi.org/10.1021/jf8011213>
- Bosetti C., Filomeno M., Riso P., Polesel J., Levi F., Talamini R., Montella M., Negri E., Franceschi S., La Vecchia C. (2012): Cruciferous vegetables and cancer risk in a network of case-control studies. *Ann. Oncol.* **23**, 2198–2203  
<http://dx.doi.org/10.1093/annonc/mdr604>
- Choi S., Singh S. V. (2005): Bax and bak are required for apoptosis induction by sulforaphane, a cruciferous vegetable-derived cancer chemopreventive agent. *Cancer Res.* **65**, 2035–2043  
<http://dx.doi.org/10.1158/0008-5472.CAN-04-3616>
- Clarke J. D., Dashwood R. H., Ho E. (2008): Multi-targeted prevention of cancer by sulforaphane. *Cancer Lett.* **269**, 291–304  
<http://dx.doi.org/10.1016/j.canlet.2008.04.018>
- Fahey J. W., Wehage S. L., Holtzclaw W. D., Kensler T. W., Egner P. A., Shapiro T. A., Talalay P. (2012): Protection of humans by plant glucosinolates: Efficiency of conversion of glucosinolates to isothiocyanates by the gastrointestinal microflora. *Cancer Prev. Res.* **5**, 603–611  
<http://dx.doi.org/10.1158/1940-6207.CAPR-11-0538>
- Giovannucci E., Rimm E. B., Liu Y. (2003): A prospective study of cruciferous vegetables and prostate cancer. *Cancer Epidemiol. Biomarkers Prev.* **12**, 1403–1409
- Gotoda T., Yanagisawa A., Sasako M., Ono H., Nakanishi Y., Shimoda T., Kato Y. (2000): Incidence of lymph node metastasis from early gastric cancer: estimation with a large number of cases at two large centers. *Gastric Cancer* **3**, 219–225  
<http://dx.doi.org/10.1007/PL00011720>
- Gupta P., Wright S. E., Kim, S., Srivastava S.K. (2014): Phenethyl isothiocyanate: A comprehensive review of anti-cancer mechanisms. *Biochim. Biophys. Acta* **1846**, 405–424  
<http://dx.doi.org/10.1016/j.bbcan.2014.08.003>
- Hartgrink H. H., Jansen E. P. M., van Grieken N. C. T., van de Velde C. J. H. (2009): Gastric cancer. *Lancet* **374**, 477–490  
[http://dx.doi.org/10.1016/S0140-6736\(09\)60617-6](http://dx.doi.org/10.1016/S0140-6736(09)60617-6)
- Ho C. C., Lai K. C., Hsu S. C., Kuo C. L., Ma C. Y., Lin M. L., Yang J. S., Chung J. G. (2011): Benzyl isothiocyanate (BITC) inhibits migration and invasion of human gastric cancer AGS cells via suppressing ERK signal pathways. *Hum. Exp. Toxicol.* **30**, 296–306

- <http://dx.doi.org/10.1177/09603271110371991>
- Inoue M., Tsugane S. (2005): Epidemiology of gastric cancer in Japan. *Postgrad. Med. J.* **81**, 419–424  
<http://dx.doi.org/10.1136/pgmj.2004.029330>
- Kaur I. P. (2009): Inhibition of cooked food-induced mutagenesis by dietary constituents: Comparison of two natural isothiocyanates. *Food Chem.* **112**, 977–981  
<http://dx.doi.org/10.1016/j.foodchem.2008.07.019>
- Lam T. K., Gallicchio L., Lindsley K., Shiels M., Hammond E., Tao X. G., Chen L., Robinson K. A., Caulfield L. E., Herman J. G., Guallar E., Alberg A. J. (2009): Cruciferous vegetable consumption and lung cancer risk: a systematic review. *Cancer Epidemiol. Biomarkers Prev.* **18**, 184–195  
<http://dx.doi.org/10.1158/1055-9965.EPI-08-0710>
- Liang C. C., Park A. Y., Guan J. L. (2007): In vitro scratch assay: a convenient and inexpensive method for analysis of cell migration in vitro. *Nat. Protoc.* **2**, 329–333  
<http://dx.doi.org/10.1038/nprot.2007.30>
- Leung W. K., Wu M. S., Kakugawa Y., Kim J. J., Yeoh K. G., Goh K. L., Wu K. C., Wu D. C., Sollano J., Kachintorn U., Gotoda T., Lin J. T., You W. C., Ng E. K., Sung J. J. (2008): Screening for gastric cancer in Asia: current evidence and practice. *Lancet Oncol.* **9**, 279–287  
[http://dx.doi.org/10.1016/S1470-2045\(08\)70072-X](http://dx.doi.org/10.1016/S1470-2045(08)70072-X)
- Mi L., Xiao Z., Hood B. L., Dakshnamurthy S., Wang X., Govind S., Conrads T. P., Veenstra T. D., Chung F. L. (2008). Covalent binding to tubulin by isothiocyanates. A mechanism of cell growth arrest and apoptosis. *J. Biol. Chem.* **283**, 22136–22146  
<http://dx.doi.org/10.1074/jbc.M802330200>
- Papi A., Orlandi M., Bartolini G., Barillari J., Iori R., Paolini M., Ferroni F., Fumo M. G., Pedulli G. F., Valgimigli L. (2008): Cytotoxic and antioxidant activity of 4-methylthio-3-butenyl isothiocyanate from *Raphanus sativus* L. (Kaiware Daikon) sprouts. *J. Agric. Food Chem.* **56**, 875–883  
<http://dx.doi.org/10.1021/jf073123c>
- Pocasap P., Weerapreeyakul N., Barusrux S. (2013): Cancer preventive effect of Thai rat-tailed radish (*Raphanus sativus* L. var. *caudatus* Alef). *J. Funct. Foods* **5**, 1372–1381  
<http://dx.doi.org/10.1016/j.jff.2013.05.005>
- Powlony A. A., Bommareddy A., Hahm E. R., Normolle D. P., Beumer J. H., Nelson J. B., Singh S. V. (2011): Chemopreventative potential of the cruciferous vegetable constituent phenethyl isothiocyanate in a mouse model of prostate cancer. *J. Natl. Cancer Inst.* **103**, 571–584  
<http://dx.doi.org/10.1093/jnci/djr029>
- Razis A. F. A., Noor N. M. (2013): Cruciferous vegetables: Dietary phytochemicals for cancer prevention. *Asian Pacific J. Cancer Prev.* **14**, 1565–1570  
<http://dx.doi.org/10.7314/APJCP.2013.14.3.1565>
- Stivarou T., Patsavoudi E. (2015): Extracellular molecules involved in cancer cell invasion. *Cancers* **7**, 238–265  
<http://dx.doi.org/10.3390/cancers7010238>
- Tournier C., Hess P., Yang D. D., Xu J., Turner T. K., Nimmual A., Bar-Sagi D., Jones S. N., Flavell R. A., Davis R. J. (2000): Requirement of JNK for stress-induced activation of the cytochrome c-mediated death pathway. *Science* **288**, 870–874  
<http://dx.doi.org/10.1126/science.288.5467.870>
- Tsuruta F., Sunayama J., Mori Y., Hattori S., Shimizu S., Tsujimoto Y., Yoshioka K., Masuyama N., Gotoh Y. (2004): JNK promotes Bax translocation to mitochondria through phosphorylation of 14-3-3 proteins. *EMBO J.* **23**, 1889–1899  
<http://dx.doi.org/10.1038/sj.emboj.7600194>
- Wu C. L., Huang A. C., Yang J. S., Liao C. L., Lu H. F., Chou S. T., Ma C. Y., Hsia T. C., Ko Y. C., Chung J. G. (2011): Benzyl isothiocyanate (BITC) and phenethyl isothiocyanate (PEITC) – mediated generation of reactive oxygen species causes cell cycle arrest and induces apoptosis via activation of caspase-3, mitochondria dysfunction and nitric oxide (NO) in human osteogenic. *J. Orthop. Res.* **29**, 1199–1209  
<http://dx.doi.org/10.1002/jor.21350>
- Wu X., Zhou Q., Xu K. (2009): Are isothiocyanates potential anti-cancer drugs? *Acta Pharmacol. Sin.* **30**, 501–512  
<http://dx.doi.org/10.1038/aps.2009.50>
- Yan H., Zhu Y., Liu B., Wu H., Li Y., Wu X., Zhou Q., Xu K. (2011): Mitogen-activated protein kinase mediates the apoptosis of highly metastatic human non-small cell lung cancer cells induced by isothiocyanates. *Br. J. Nutr.* **106**, 1779–1791  
<http://dx.doi.org/10.1017/S0007114511002315>
- Yang M. D., Lai K. C., Lai T. Y., Hsu S. C., Kuo C. L., Yu C. S., Lin M. L., Yang J. S., Kuo H. M., Wu S. H., Chung J. G. (2010): Phenethyl isothiocyanate inhibits migration and invasion of human gastric cancer AGS cells through suppressing MAPK and NF- $\kappa$ B signal pathways. *Anticancer Res.* **30**, 2135–2143
- Zhang L., Chen W., Li X. (2008): A novel anticancer effect of butein: Inhibition of invasion through the ERK1/2 and NF- $\kappa$ B signaling pathways in bladder cancer cells. *FEBS Lett.* **582**, 1821–1828  
<http://dx.doi.org/10.1016/j.febslet.2008.04.046>
- Zhang Y. (2004): Cancer-preventive isothiocyanates: Measurement of human exposure and mechanism of action. *Mutat. Res.* **555**, 173–190  
<http://dx.doi.org/10.1016/j.mrfmmm.2004.04.017>

Received: May 7, 2015

Final version accepted: July 30, 2015

First published online: November 27, 2015